Bio-Medical Materials and Engineering 26 (2015) S1677–S1683
DOI 10.3233/BME-151467
IOS Press

In vivo evaluating skin doses for lung cancer patients undergoing volumetric modulated arc therapy treatment

Hsien-Chun Tseng[a,b], Lung-Kang Pan[c], Hsin-Yu Chen[d], Wen-Shan Liu[e], Chang-Chieh Hsu[d,f] and Chien-Yi Chen[d,*]

[a]*Department of Radiation Oncology, Chung Shan Medical University Hospital, Taiwan, Republic of China*
[b]*School of Medicine, Chung Shan Medical University, Taichung 40201, Taiwan, Republic of China*
[c]*Graduate Institute of Radiological Science, Central Taiwan University of Science and Technology, Takun, Taichung 40609, Taiwan, Republic of China*
[d]*School of Medical Imaging and Radiological Sciences, Chung Shan Medical University, Taichung 40201, Taiwan, Republic of China*
[e]*Department of Radiation Oncology, Kaohsiung Veterans Geeral Hospital, Kaohsiung 81362, Taiwan, Republic of China*
[f]*Department of Biomedical Imaging and Radiological Sciences, National Yang-Ming University, Taipei, 11221 Taiwan, Republic of China*

Abstract. This study is the first to use 10- to 90-kg tissue-equivalent phantoms as patient surrogates to measure peripheral skin doses (D_{skin}) in lung cancer treatment through Volumetric Modulated Arc Therapy of the Axesse linac. Five tissue-equivalent and Rando phantoms were used to simulate lung cancer patients using the thermoluminescent dosimetry (TLD-100H) approach. TLD-100H was calibrated using 6 MV photons coming from the Axesse linac. Then it was inserted into phantom positions that closely corresponded with the position of the represented organs and tissues. TLDs were measured using the Harshaw 3500 TLD reader. The ICRP 60 evaluated the mean D_{skin} to the lung cancer for 1 fraction (7 Gy) undergoing VMAT. The D_{skin} of these phantoms ranged from 0.51±0.08 (10-kg) to 0.22±0.03 (90-kg) mSv/Gy. Each experiment examined the relationship between the D_{skin} and the distance from the treatment field. These revealed strong variations in positions close to the tumor center. The correlation between D_{skin} and body weight was D_{skin} (mSv) = -0.0034x + 0.5296, where x was phantom's weight in kg. R^2 is equal to 0.9788. This equation can be used to derive an equation for lung cancer in males. Finally, the results are compared to other published research. These findings are pertinent to patients, physicians, radiologists, and the public.

Keywords: Axesse linac, skin dose, TLD, tissue-equivalent phantom, ICRP 60

* Address for correspondence: Chien-Yi Chen, School of Medical Imaging and Radiological Sciences, Chung Shan Medical University, Taichung 40201, Taiwan, Republic of China. Tel.: 886-928661433; Fax: 886-928661433; E-mail: ccy@csmu.edu.tw.

1. Introduction

The medical linear accelerator (linac), Axesse (Elekta Inc, Maryland, USA), can provide photon energies with accelerating voltages of 6 MV that can deliver Volumetric Modulated Arc Therapy (VMAT). VMAT is a powerful technique for irradiating many treatment sites and obtaining higher dose conformity to the tumor; it also decreases intra-fraction movements because of its shorter delivery times [1]. During treatment, the patient was exposed to significantly undesirable radiation that was primarily caused by out-of-field radiation resulting from collimators and beam modifiers. It is necessary to estimate the accompanying extra radiation to estimate the (peripheral) skin doses (D_{skin}) for patients. The peripheral dose was defined as the radiation dose anywhere outside the treatment field; it was composed of the scatter dose and the leakage dose. These authors are aware of no studies assessing D_{skin} that results from differences in patient weights from the linac; no comparisons can be made between previous studies of the D_{skin} of different body-weights for VMAT lung cancer treatment [2, 3]. However, the D_{skin} is a matter of concern. This study is the first to develop different body-weight indigenous tissue-equivalent phantoms as patient surrogates, ranging from 10- to 90-kg, using thermoluminescent dosimetry (TLD-100H) (3.0×3.0×1.0 mm^3, Harshaw, OH, USA) [4, 5]. Intensive efforts should establish a more reliable and practical method for quantitative measurement of patients' D_{skin}, to effectively provide the data to improve radiation safety.

2. Material and methods

2.1. Tissue-equivalent phantom

This study developed five tissue-equivalent phantoms of 10-, 30-, 50-, 70-, and 90-kg. Anthropometric-shaped skeletons constructed from epoxy-resin and polymethylmethacrylate (PMMA) were used to simulate patients [4, 6]. The phantom was designed based on the GSF-Forshungszentrum fur Umwelt und Gesundheit (Germay) adult mathematical models, and the lung masses were based on the ICRP reference man [4, 7]. The materials' densities are as follows: the lung tissue-equivalent was 0.296, the skeleton-cortical-bone tissue-equivalent was 1.486, and the skin tissue-equivalent was 1.105 g/cm^3 [4, 6]. The phantom was based on the general human design. Each was comprised of 31 slices, representing the head, neck, torso and abdomen, but without arms or legs [4, 6]. Table 1 lists the dimensions and physical properties of the Rando and tissue-equivalent phantoms [4].

The Rando phantom (Alderson Radiation Therapy Phantom, Radiology Support Devices, Long Beach, CA) is suitable for oncology dose measurements [4]. Figure 1 shows the outer appearance of the five tissue-equivalent and Rando phantoms.

2.2. Dosimetry

A total of 31 measurement positions were selected on the anterior central line and are marked as 1-

Table 1

Dimension and physical properties of Rando, tissue-equivalent phantoms

Phantom	Rando	Tissue-equivalent				
Weight (kg)[1]	70	10	30	50	70	90
Height (cm)[2]	94.5	50	78	84	93	112
Weight (kg)[2]	34.5	6.75	19.0	31.5	44.1	57
cm $slices^{-1}$	2.5	1.6	2.3	2.7	3.0	3.6

Note: [1]original design referred from ICRU 48; [2]without arms and legs.

Fig. 1. Use five tissue-equivalent and Rando phantoms as patient surrogates.

Fig. 2. Illustration of the 70-kg phantom with the TLD measurement positions marked.

31 in Figure 2. Accordingly, since the $D_{skin,\,i}$ of each slice is different, the average D_{skin} (i = 1-31) of the *i*th slice was computed, and $D_{skin,\,i}$ was substtuted into Eq. (1). The D_{skin} was determined by adding the D_i of all scan slices and weighting each with its absorbed dose. D_{skin}, was evaluated from the equation:

$$D_{skin} = \frac{\sum D_{skin,i}}{31} \quad (i = 1 \sim 31) \tag{1}$$

where $D_{skin,\,i}$ is the absorbed dose for phantoms at each slice. These measured TLD were presented the D_{skin} distributions of phantoms [8].

The TLDs were analyzed using a fully automated Harshaw 3500 reader (Bicron NE, Solon, OH). The element correction coefficient determined the relative sensitivity of these TLDs to correct the variation of each batch's individual sensitivity. All TLDs were pre-annealed at 240°C for 10 min in a microprocessor-controlled oven via a Barnstead/Thermolyne 47900 Furnace (Thermolyne Co.), followed by a rapid cooling on an aluminum block [4, 5, 9].

2.3. Calibrated TLD-100H using 6MV beams

The TLD-100H was selected for its small dimensions and the response's lower dependence on phton energy, dose rate, and the radiation's direction of incidence. The TLDs were irradiated according to the International Atomic Energy Agency recommendations (TRS-398) by placing the mover on five solid water phantom (SWP) slabs, 30×30 cm^2 in area and 10 mm in thickness, for electronic equilibrium, and then placing a SWP above them, using a skin source distance (SSD) of 100 cm and a 10×10 cm^2 field [4, 5]. As in other studies, a Farmer-type ionization chamber, type NE 2571 (PTW, Freiburg, UNIDOS), which had a volume of 0.6 cc, was positioned in the solid water [4, 5].

2.4. CT simulation and treatment plan of lung cancer

All the computed tomography (CT) images (GE Aquillion 64, Toshiba Medical Solutions, Japan) of the phantoms were transferred and registered in the treatment planning system [1, 2, 10-13]. Phantoms were introduced into a CT-based simulation in a supine position. Lung treatment plans with Axesse were developed and reviewed by professional medical doctors (Hsien-Chun Tseng, MD) and senior radiotherapists (Hsin-Yi Chu), both with 10 years of experience [4, 6]. The target volume in the 70-kg phantom's lung was 64 cm^3 at a depth of 5 cm. A marker was used to place skin marks in three directions [1, 2, 14]. Figure 3(a) shows the treatment plan of the Pinnacle planning system (Philips

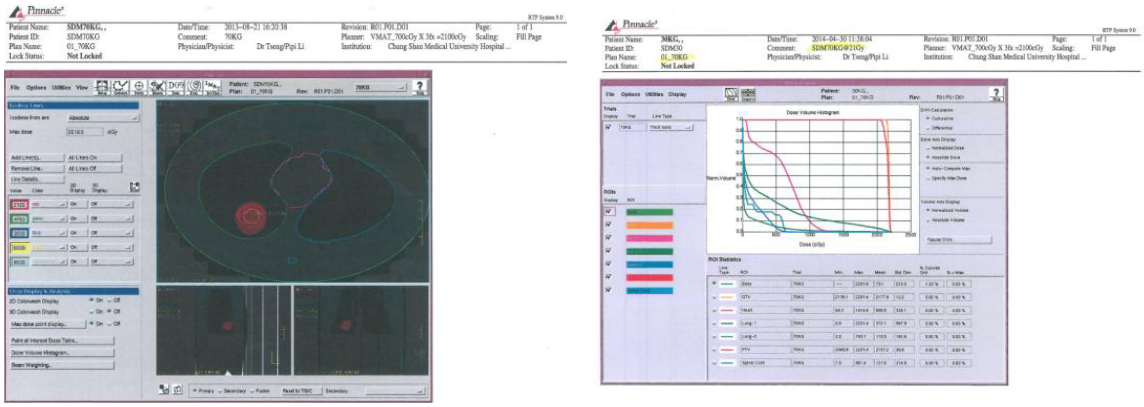

(a) (b)

Fig. 3. (a) The treatment plan of Pinnacle planning system of 70-kg tissue-equivalent phantom; (b) Isodose distributions of the 30-kg tissue-equivalent phantom.

Radiation Oncology System, Fitchburg, WI, USA) of the 70-kg tissue-equivalent phantom, and Figure 3(b) shows the isodose distributions of the 30-kg tissue-equivalent phantom.

The CT images and organ contours were transferred for VMAT at the Department of Radiation Oncology at Chung Shan Medical University Hospital (CSMUH) in Taichung ROC. The prescribed dose was specified at the planning target volume (PTV). Complete prescribed photo doses (700 cGy) of 6 MV were showed in red and delivered to the phantom's PTV in a single treatment.

The protocol required a total dose of 21 Gy to the tumor. Organs at risk are marked as follows: heart (red colorwash); lung 1 (green colorwash); lung 2 (blue colorwash); and spinal cord (cyanine colorwash). The prescribed isodose (21 Gy) is shown in red.

2.5. In vivo measurement during VMAT

In vivo measurements were mainly located in the skin. The primary irradiation and extra radiation were measured first in the skin, and then throughout the body. Ninety three of the TLDs were attached to these phantoms at each slice. One-bag of TLDs were inserted into the tumor's center to directly evaluate the tumor dose at the 12th slice. For all locations, the final D_{skin} was obtained by averaging the three TLDs of each slice [4, 9]. Nine TLD chips were used to measure background radiation at our low-background lab. For each measurement slice, three individually calibrated TLDs packed into one bag yielded three readings. These were averaged to obtain the TLD-measured doses for measuring $D_{skin,\,i}$ [4]. The error bars represent the uncertainty of the D_{skin} values across the different TLDs in a same slice.

3. Results and discussions

3.1. Uncertainty

The precision and accuracy of the TLD-100H included several parameters, including: 1) TLD counting statistical errors ranging from 3 to 10%, 2) TLD calibrations of 6 MV photons' dose-associated nonlinearity of about 8%, 3) systematic uncertainties ranging from 3 to 8% from the

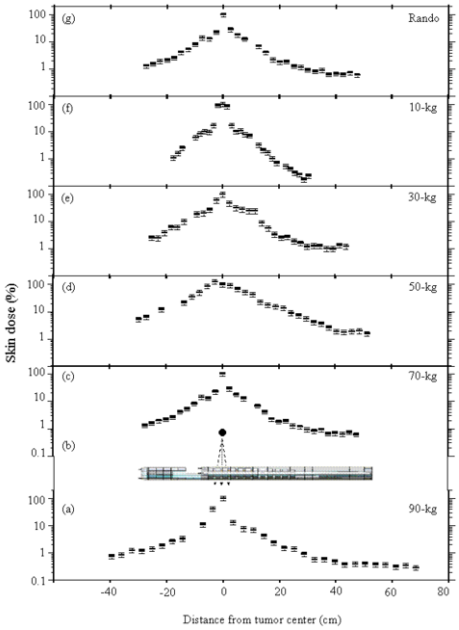

Fig. 4. Assessing the D_{skin} (mSv/Gy) distributions on six phantoms undergoing lung cancer treatment of the Axesse (a) 90-kg (b) 70-kg irradiation, TLDs inserted into the phantom, (c) 70-kg, (d) 50-kg, (e) 30-kg, (f) 10-kg, (g) Rando phantoms.

Harshaw 3500 reader, and 4) errors in power fluctuation that came from the Axesse linac were quoted based on monthly clinical quality assurance (QA) less than ± 2%. The total uncertainties ranged from 9.27 to 15.2%

3.2. Skin doses (D_{skin})

Figures 4(a)-4(g) show the *in vivo* D_{skin} based on the distance from the irradiated tumor center of the phantoms, averaged over a total of five trials. For each phantom, the D_{skin} was normalized independently to 100% of the tumor center dose. Additionally, the D_{skin} that fell off of the treatment plan, outside the scan field displayed, varied significantly and decreased as distance from the tumor center increased. It should be noted that contribution of the $D_{skin,\ 14}$ from the 14th slice of Rando phantom remarkably decreased from 100% to 7.73%.

The D_{skin} for the lung cancer treatment exposed to the 6 MV linac indicated large values, reaching up to 0.34±0.04 mSv/Gy for the Rando phantom and 0.51±0.06 (10-kg), 0.41±0.06 (30-kg), 0.35±0.05 (50-kg), 0.31±0.03 (70-kg), and 0.22±0.04 (90-kg) mSv/Gy for the tissue-equivalent phantoms of the ICRP 60 [3, 7]. Eq. (2) formulates the regression equation-linking dose with the phantoms' body-weights.

$$D_{skin}\,(\text{mSv/Gy}) = -0.0034 \times M\,(\text{kg}) + 0.5296,\ R^2 = 0.9788 \quad (2)$$

Where the D_{skin} was in the mSv/Gy, *M* denotes the tissue-equivalent phantoms in kg. Figure 5 compares the results of the D_{skin} of the 70-kg and Rando phantoms. The D_{skin} of the 70-kg phantom is 0.31±0.05 mSv/Gy, nearly 0.91 times that of the Rando phantom, at 0.34±0.04 mSv/Gy. The deviation was investigated by the density effect. The highest TLD value was obtained in the 12th slice of the

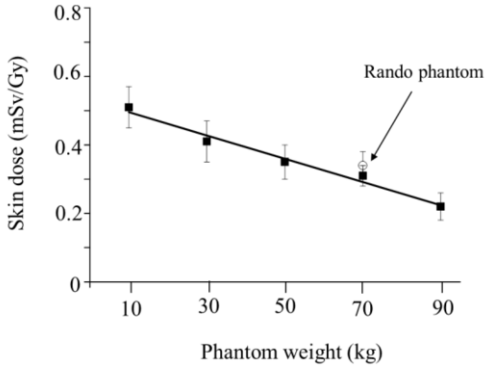

Fig. 5. Estimates of the D_{skin} (mSv/Gy) undergoing lung cancer of the Axcess linac. The average values and the spread over different TLDs are shown (bars).

phantom at 99.8±16.9% of the tumor center, and the lowest D_{skin} was determined in the TLD in slices 27 to 31, which was 0.51±0.09 % of the tumor center.

The *in vivo* measurements showed that the D_{skin} was dependent on the phantom's weight. The 10-kg phantom's is steeper than the other phantoms'. This indicates that the 10-kg phantom has a relatively high D_{skin}, due to the skin close to the tumor center.

3.3. Comparison with other studies of similar investigation types

Dr. Jia showed that the IMRT leakage dose is approximately 6 cGy, and it is uniformly distributed throughout the patient's skin, while the leakage dose from the RapidArc is about 3 cGy with a prescribed dose of 45 Gy [1]. This result fully supports our measurements [1]. In a recent paper, Dr. Tyan used a patient to evaluate *in vivo* doses of multi-slice computed tomography in abdominal examinations taken by 40- and 64 detector scanners, in-of-plane for males, and by 1.4 to 9.6 mSv (mean dose, 4.1 mSv) for females. His results were higher than those of D_{skin} ranged from 0.51±0.08 (10-kg) to 0.22±0.03 (90-kg) mSv/Gy herein, primarily due to the higher dose conformity to the tumor and the rapid decrease of VMAT of the Axcess linac [8].

The different results obtained from the above-mentioned studies can be attributed to the differences: (A) in treatment modalities, (B) in the TLDs' distance from the tumor center, (C) in measured approaches, and (D) in linac performance. Additionally, other differences may arise from density inconsistencies between the tissue-equivalent and the anthropomorphic phantoms used. This may be true despite the fact that the specified densities of the tissue-equivalent phantoms are close to Rando phantom. However, these phantoms and the TLD approach can be a useful and reliable method for D_{skin} estimations.

4. Conclusion

The *in vivo* D_{skin} measurements reveal a measurable difference between tissue-equivalent phantoms that involving extra peripheral radiations. Among all the phantoms, the 10-kg SDM has the highest D_{skin}. The D_{skin} reached up to 0.34±0.04 mSv/Gy for the Rando phantom. The closer it is to tumor center; the higher dose the skin will receive. The calculated $D_{skin,\,i}$ clearly show that $D_{skin,}$ decreases with increasing distance. The D_{skin} was highest near the tumor center and decreased with distance from

the tumor center. The D_{skin} decreased in an inverse correlation with increasing phantom weight. There was good linearity between each TLD. The highest TLD value was obtained in the 12^{th} slice of the phantom at 99.8±16.9% of the tumor center. These results indicate that the TLD-100H approach displays high sensitivity and stability. The reported *in vivo* D_{skin} measurements demonstrate that tissue-equivalent phantoms designed using ICRU 48 can provide a reliable method for evaluating D_{skin} radiations as well as applicable for other cancer, such as, lung cancer, head and neck cancer. The quantitative results can provide practical guidance regarding radiation protection.

Acknowledgments

The authors would like to thank the radiotherapists of CSMUH for their efficient supports. Financial assistances were partly supported by the CSMU under Contract No. CSMU-INT-102-08 and Ministry of Science and Technology of the Republic of China under Contract No. MOST-103-2314-040-003.

References

[1] M.X. Jia, X. Zhang, C. Yin, G. Feng, N. Li, S. Gao and D.W. Liu, Peripheral dose measurements in cervical cancer radiotherapy: A comparison of volumetric modulated arc therapy and step-and-shoot IMRT techniques, Radiation Oncology **9** (2014), 61–67.
[2] L. Zhou, L.H. Zhou, S. Zhang, X. Zhen, H. Yu, G.Q. Zhang and R.H. Wang, Validation of an improved 'diffeomorphic demons' algorithm for deformable image registration in image-guided radiation therapy, Bio-Medical Materials and Engineering **24** (2014), 373–382.
[3] Z. Zhou, Y. Chen, Z. Yu, D. Wang, C. Zhao, J. Xu, W. Song, B. Li, J. Shen and X. Zhu, A study of quality control method for IMRT planning based on prior knowledge and novel measures derived from both OVHs and DVHs, Bio-Medical Materials and Engineering **24** (2014), 3479–3485.
[4] S.Y. Tsai, C.Y. Chen and J.C. Chen, Evaluating effective dose for indigenous phantoms with different weights undergoing computed tomography examination for coronary artery calcium, IEEE Transactions on Nuclear Science **60** (2013), 2147–2154.
[5] G. Tanir, F. Cengiz and M.H. Bolukdemir, Measurement of dose given by Co-60 in radiotherapy with TLD-500, Radiation Physics and Chemistry **81** (2012), 355–357.
[6] International Commission on Radiation Units and Measurements, ICRU report 48: Phantoms and computational models in therapy, diagnosis and protection, International Commission on Radiation Uuits and Measurements, 1992.
[7] ICRP Publication 60, 1990 recommendations of the international commission on radiological protection technical report ICRP-60, International Commission on Radiological Protection 21 (1991).
[8] Y.S. Tyan, H.Y. Tsai, Y.L. Hung, N.G. Lia and C.P. Chen, In vivo dose assessment of multislice CT in abdominal examinations, Radiation measurement **43** (2008), 1012–1016.
[9] C. Kawaura, T. Aoyama, S. Koyama, M. Achiwa and M. Mori, Organ and effective dose evaluation in diagnostic radiology based on in-phantom dose measurements with novel photodiode-dosemeters, Radiation Protection Dosimetry **118** (2006), 421–430.
[10] H. Li, K. Liu, H. Sun, N. Bao, X. Wang, S. Tian, S. Qi and Y. Kang, Automatic heart positioning method in computed tomography scout images, Bio-Medical Materials and Engineering **24** (2014), 3277–3286.
[11] H. Yu, S.X. Zhang, R.H. Wang, G.Q. Zhang and J.M. Tan, The feasibility of mapping dose distribution of 4DCT images with deformable image registration in lung, Bio-Medical Materials and Engineering **24** (2014), 145–153.
[12] S.X. Zhang, P.H. Han, G.Q. Zhang, R.H. Wang, Y.B. Ge, Z.G. Ren, J.S. Li and W.H. Fu, Comparison of SPECT/CT, MRI and CT in diagnosis of skull base bone invasion in nasopharyngeal carcinoma, Bio-Medical Materials and Engineering **24** (2014), 1117–1124.
[13] S.X. Zhang, L.H. Zhou, S.Q. Lin, H. Yu, G.Q. Zhang, R.H. Wang and B. Qi, 4D-CT reconstruction based on pulmonary average CT values, Bio-Medical Materials and Engineering **24** (2014), 85–94.
[14] N. Bao, Y. Chen, Y. Yu, H. Li, Z. Cui. J. Zhuang, S. Tian and Y. Kang, Fiducial markers configuration optimization in image-guided surgery Bio-Medical Materials and Engineering **24** (2014), 3361–3371.